

## Dependence of lithium–zinc ferrosphel phase composition on the duration of synthesis in an accelerated electron beam

A. P. Surzhikov · A. M. Pritulov · E. N. Lysenko ·  
A. N. Sokolovskii · V. A. Vlasov · E. A. Vasendina

Received: 12 July 2011 / Accepted: 21 September 2011 / Published online: 11 October 2011  
© Akadémiai Kiadó, Budapest, Hungary 2011

**Abstract** Kinetic changes in the phase composition of the  $\text{Li}_2\text{CO}_3\text{--Fe}_2\text{O}_3\text{--ZnO}$  system are investigated by the methods of X-ray phase and TG/DTG analysis. The powder mixture components were in the ratio corresponding to  $\text{Li}_{0.4}\text{Fe}_{2.4}\text{Zn}_{0.2}\text{O}_4$  ferrite. The synthesis was performed by thermal heating of mixture reagents in a furnace and heating of the mixture upon exposure to high-power beam of accelerated electrons with energy of 2.4 MeV. It is demonstrated that the sequence of phase formation is independent of the heating method. The radiative effect of synthesis intensification is most strongly manifested in the initial stage of forming lithium monoferrite phases. The rate of diffusion interaction of intermediate phases also increases upon exposure to the electron beam in the stage of end-product formation.

**Keywords** Li–Zn ferrite · Pulsed electron beam · Radiation-thermal method · Solid-state synthesis · TG/DTG analysis

### Introduction

The solid-state synthesis is the main method of commercial production of microwave ferrites. However, the efficiency of the given classical method sharply decreases when manufacturing multicomponent ferrite powders. This is caused by the fact that the mechanical mixture of reagents consists of different oxides, and ferrite formation starts in

regions of their contact. Therefore, the primary products of solid-phase reactions in this stage are conventionally monoferrites and oxide solid solutions. All this causes the primary products of solid phase reactions to differ by their chemical composition whose fluctuations are retained during further annealing. Because of inhomogeneity of the reaction mixture, repeated alternation of grinding and thermal treatment operations is often performed for completeness of solid-phase reactions, thereby significantly increasing the time of synthesis. In addition, a serious disadvantage of repeated grinding is getting into the reaction mixture of mill material that adversely affects the properties of the material obtained.

The developers try to increase the efficiency of solid-phase synthesis by application of special methods influencing the solid-phase systems that allow the reagents to be activated directly in the process of synthesis. Among these methods are mechanochemical [1], microwave [2], and sonochemical [3, 4] treatment of the reaction mixtures.

In [5, 6] it was demonstrated that heating of materials by a high-power flow of accelerated electrons is an efficient method of intensification of solid-phase interactions. This method is called radiation-thermal (RT), because it combines simultaneous influence of thermal and radiation factors. The advantage of the given method of heating is the rapidity and low iteration of material heating, absence of contact between the heated body and the heater, and homogeneity of material heating throughout the volume. Unlike microwave exposure, the dielectric properties of materials have no effect on electron irradiation.

The efficiency of the RT method of lithium compound synthesis was established in [9–12]. However, the results presented there were limited in character, since they were obtained either for simple binary  $\text{Li}_2\text{CO}_3\text{--Fe}_2\text{O}_3$  systems [9] or ternary  $\text{Li}_2\text{CO}_3\text{--Fe}_2\text{O}_3\text{--ZnO}$  systems, but for a

A. P. Surzhikov · A. M. Pritulov · E. N. Lysenko (✉) ·  
A. N. Sokolovskii · V. A. Vlasov · E. A. Vasendina  
Tomsk Polytechnic University, 30, Lenin Avenue,  
Tomsk, Russia 634050  
e-mail: lysenkoen@tpu.ru

particular annealing regime ( $T = 700\text{ }^{\circ}\text{C}$  and  $t_{\text{ann}} = 120\text{ min}$ ) [10–12].

In this study, we investigate the kinetic transformations of the phase composition in the ternary  $\text{Li}_2\text{CO}_3\text{--Fe}_2\text{O}_3\text{--ZnO}$  system after thermal ( $T$ ) and RT annealing of reaction mixtures at temperatures of 600 and 750  $^{\circ}\text{C}$ . When choosing the object of research, we took into account that alloyed lithium ferrites are important materials of modern microwave technology [7, 8].

## Experimental

Lithium–zinc ferrite samples were prepared from the mechanical mixture of  $\text{Li}_2\text{CO}_3\text{--Fe}_2\text{O}_3\text{--ZnO}$  powders. The composition of mixtures corresponded to the formula  $\text{Li}_{0.4}\text{Fe}_{2.4}\text{Zn}_{0.2}\text{O}_4$ . Samples were compacted by single-ended cold pressing under a pressure of 200 MPa in the form of tablets with a diameter of 15 mm and thickness of 2 mm. Then samples were subdivided into two groups to study the processes of synthesis at  $T$  and RT annealing.

Thermal annealing of samples was performed in a resistance furnace. Radiation-thermal annealing of samples was carried out in an ILU-6 pulse electron accelerator (Institute of Nuclear Physics of the SB RAS, Novosibirsk, Russia). The electron energy was 2.4 MeV, the beam current in the pulse was 400 mA, the pulse duration was 500  $\mu\text{s}$ , and the pulse repetition frequency was 7–15 Hz. The average radiation dose was  $\sim 5\text{ kGy s}^{-1}$  at heating and  $\sim 3\text{ kGy s}^{-1}$  at isothermal annealing. The pulse radiation dose was 800  $\text{kGy s}^{-1}$ . The samples were heated and the preset temperature regime was maintained at the expense of energy of decelerated electrons without external heat sources. The duration of non-isothermal stages (heating and cooling) did not exceed 3 min. Both annealing methods were realized in air, without intermediate grinding and mixing.

The phase composition of the examined samples was measured using an ARL X'TRA X-ray diffractometer (Switzerland) with a Peltier Si(Li) semiconductor detector and Cu  $K_{\alpha}$  radiation. XRD patterns were measured for  $2\theta = (10\text{--}140)^{\circ}$  with a scan rate of  $0.02^{\circ}/\text{s}$ .

The phase composition of the examined samples was determined using the PDF-4 powder database of the International Centre for Diffraction Data (ICDD). The XRD patterns were processed by the full-profile analysis using the software *Powder Cell 2.5*. To analyze the phase composition of ferritized samples, a discrete set of lithium–zinc ferrite phases with  $x_{\text{Zn}} = 0, 0.2, 0.4, 0.6,$  and  $0.8$  was included in the program of full-profile analysis. The given set reflected quasi-continuous distribution of  $\text{Li}_{0.5(1-x)}\text{Zn}_x\text{Fe}_{2.5-0.5x}\text{O}_4$  type spinel phases that could be formed in different regions of the powder mixture. When needed, the discrete set could

be expanded at the expense of inclusion of phases of particles of the initial components. After termination of fitting of the calculated and experimental XRD patterns, the concentration of phases, and the parameters of their crystal lattices were determined. Then, using the dependence of the lithium–zinc ferrite lattice parameters on the zinc content [14],  $x_{\text{Zn}}$  values were refined for the spinel phases. The refined  $x_{\text{Zn}}$  values are actually the average ones that characterize the distribution of lithium–zinc ferros spinel phases [12].

The thermogravimetric and calorimetric TG/DSC investigations were performed in the air atmosphere using an STA 449C Jupiter thermal analyzer (Netzsch, Germany). To control the sample magnetic state, permanent magnets creating a field of  $\sim 5\text{ Oe}$  were placed on the external side of the measuring cell. Measurements were carried out in the mode of linear cooling at a rate of  $20\text{ }^{\circ}\text{C}/\text{min}$  after the samples had been heated fast to  $800\text{ }^{\circ}\text{C}$ . Such measurement mode provided the initial demagnetized state of the samples. The thermogravimetric method of registration of the magnetic phases in the presence of an external magnetic field has already been used to investigate some materials [13].

## Results and discussion

### X-ray diffraction analysis

X-ray powder diffraction patterns of ferritized mixtures, as a rule, represent a superposition of reflections from spinel phases and from particles of the initial  $\text{ZnO}$  and  $\text{Fe}_2\text{O}_3$  oxides. The relative content of phases depends on the annealing duration, temperature, and type. Figure 1 shows results of identification of spinel compounds in the mixture ferritized in  $T$  and RT annealing regimes at a temperature of  $600\text{ }^{\circ}\text{C}$ . The type and duration of isothermal annealing

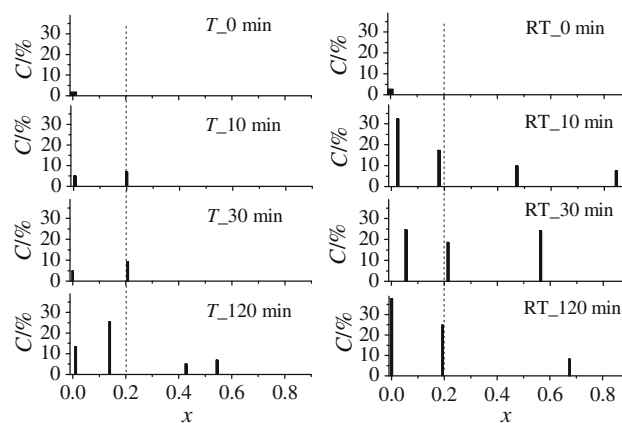


**Fig. 1** Concentration of the  $\text{Li}_{0.5(1-x)}\text{Zn}_x\text{Fe}_{2.5-0.5x}\text{O}_4$  spinel phases in reaction mixtures for the indicated duration of  $T$  and RT annealing at a temperature of  $600\text{ }^{\circ}\text{C}$

are indicated in the figure. The dashed straight lines indicate the preset mixture composition with  $x = 0.2$ .

From the XRD patterns it can be seen that during thermal annealing, the synthesis of spinel phases starts with the formation of  $\text{Li}_{0.5}\text{Fe}_{2.5}\text{O}_4$  lithium pentaferriite and lithium–zinc ferrite with  $x \sim 0.2$ . With increasing annealing time, the concentrations of these phases also increase. The concentrations of phases with high zinc content increase simultaneously.

The same sequence of stages of phase formation, but with much higher rate of the processes was observed during synthesis in an electron beam. This follows from the fact that already after annealing for 10 min, the concentrations of  $\text{Li}_{0.5}\text{Fe}_{2.5}\text{O}_4$  and phases close to it exceed three times the pentaferriite concentration after thermal annealing for 120 min. During RT annealing, phases with high zinc content, including phases with preset composition, are formed much earlier. Moreover, in the final stage of RT annealing ( $t_{\text{ann}} = 120$  min), the spectrum of spinel ferrite phase composition is simplified, which indicates the onset of mixture homogenization under conditions of RT annealing.

An increase in the ferritization annealing temperature to  $750^\circ\text{C}$  (Fig. 2) considerably increases the rate of thermal synthesis, which is manifested through the increased total concentration of spinel phases. For isothermal  $t_{\text{ann}} \geq 10$  min, spinels with  $x = 0$  and  $x = 0.15$  prevail. However, during further annealing, the concentration of these ferrites remains virtually unchanged. The amount of spinels with increased zinc content considerably increases.

After ferritization in the electron beam, greater differences in the phase composition and its kinetic changes are observed. First, in the stage of sample heating to the isothermal annealing temperature ( $t_{\text{ann}} = 0$ ), the  $\text{Li}_{0.5}\text{Fe}_{2.5}\text{O}_4$  concentration reaches its maximum of  $\sim 20\%$ , and for  $t_{\text{ann}} > 10$  min, it starts to decrease. Second, the  $\text{Li}_{0.4}\text{Fe}_{2.4}\text{Zn}_{0.2}\text{O}_4$  lithium–zinc ferrite

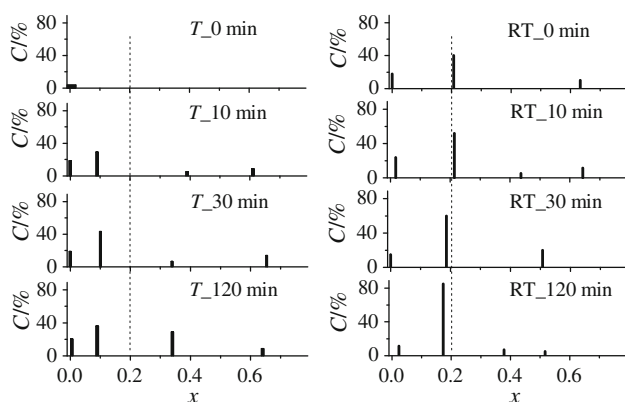


**Fig. 2** Concentration of the  $\text{Li}_{0.5(1-x)}\text{Zn}_x\text{Fe}_{2.5-0.5x}\text{O}_4$  spinel phases in reaction mixtures for the indicated duration of  $T$  and RT annealing at a temperature of  $750^\circ\text{C}$

phase whose concentration increases with increasing annealing time starts to prevail in the spinel composition. For  $t_{\text{ann}} = 120$  min, its concentration reaches 80%.

The variable character of the mixture phase composition does not allow us to estimate directly the radiation effect of synthesis acceleration from the yield of the reaction end-product. However, the notion of the degree of initial reagent transformation into the solid-phase reaction products can be used for this purpose. Figure 3 shows kinetic dependences of the degree of transformation  $\alpha$  for the components of the ZnO and  $\text{Fe}_2\text{O}_3$  reaction mixtures.

Here  $\alpha = 1 - C(t)/C_0$ , where  $C_0$  is the initial oxide concentration in the mixture. The dependences represent a superposition of the fast initial and slow linear stages of reagent consumption. From Fig. 3 it can be seen that the reagents are mainly spent on the participation in solid-phase reactions in the fast initial ( $t_{\text{ann}} \leq 30$  min) annealing stages, including non-isothermal heating of the mixture. In this stage of annealing, the radiation-induced intensification of phase formation is most strongly pronounced. The presence of two stages indicates two dominating processes of spinel phase formation. Considering that the initial rate of  $\text{Li}_{0.5}\text{Fe}_{2.5}\text{O}_4$  synthesis sharply increases during mixture heating by the electron beam [9], the initial stage can be associated with the formation of pure lithium pentaferriite phases and pentaferriite phases weakly doped with zinc. In the slow stage, the  $\text{Li}_{0.5}\text{Fe}_{2.5}\text{O}_4$  phases are enriched with zinc, and reactions of initially formed phases take place. As a result, the observed spectra of lithium and zinc monoferrite solid solutions are formed. It should be noted that in this stage, the electron beam, by analogy with the temperature, stimulates effectively the solid-phase processes.

### Thermoanalytical measurements

Results of the XRPA are confirmed and supplemented by the data of thermal analysis of the mixtures subjected to preliminary ferritization annealing either in the furnace or

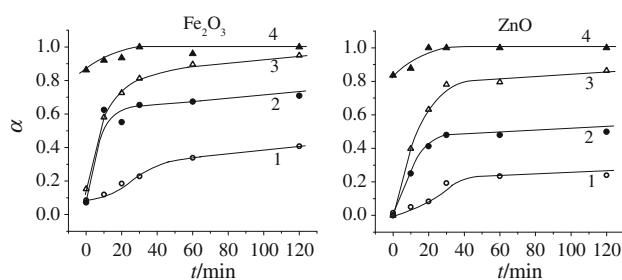
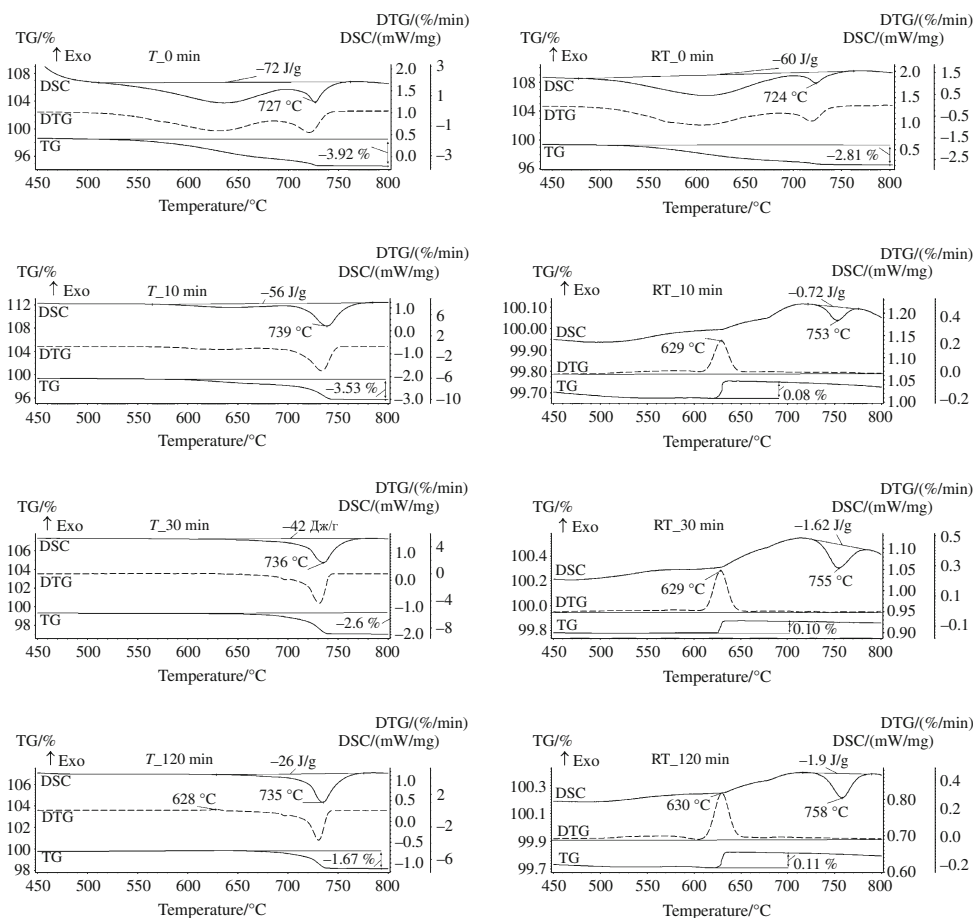


**Fig. 3** Dependences of the degree of transformation of the initial reaction mixture oxides on the duration of  $T$  (curves 1 and 3) and RT (curves 2 and 4) annealing at a temperature of  $600^\circ\text{C}$  (curves 1 and 2) and  $750^\circ\text{C}$  (curves 3 and 4)

**Fig. 4** Dependences of TG/DSC curves for reactionary mixtures after  $T$  and RT ferritization at 600 °C



in the electron beam at temperatures of 600 °C (Fig. 4) and 750 °C (Fig. 5).

The weight and thermal changes of TG/DSC curves of mixtures for 600 °C without isothermal annealing ( $t_{\text{ann}} = 0$ ) are correlated and are caused by the two-stage decomposition of lithium carbonate. The two-stage decomposition was also observed during synthesis of lithium ferrite from the mixture of lithium carbonate and iron oxide [1]. The maximum rate of the second stage coincided with the temperature of lithium carbonate melting equal to 730 °C [15, 16].

From a comparison of the total mass losses of 3.92% for  $T$  and 2.81% for RT annealing with the calculated mass loss of 3.95% it can be seen that the residual concentration of lithium carbonate after RT annealing is smaller than after  $T$  annealing, that is, mixture heating by the electron beam causes deeper decomposition of lithium carbonate. The similar conclusion follows from a comparison of the thermal effects. The increased duration of  $T$  annealing naturally reduces the residual content of lithium carbonate. Because of the masking effects of lithium carbonate decomposition, no direct evidence of lithium pentaferriite phase occurrence was revealed.

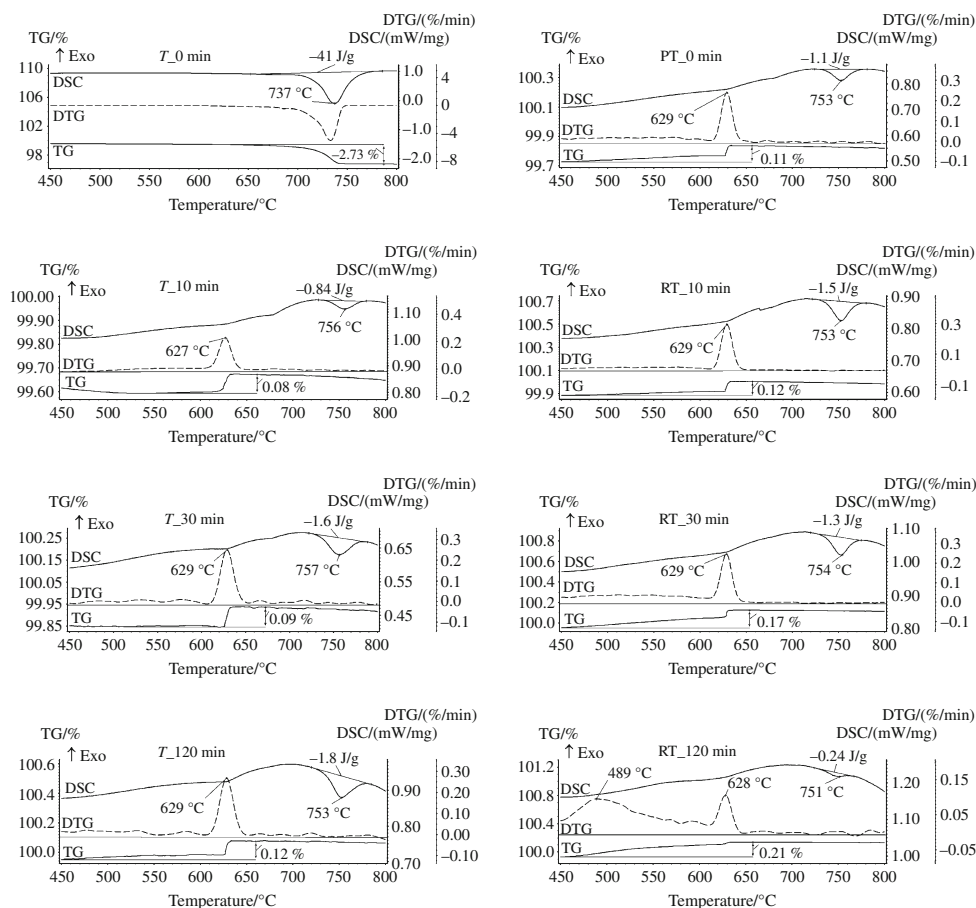
Radiation-thermal ferritization whose duration is 10 min or longer leads to qualitative changes of the TG/DSC dependences:

First, mixture annealing in the electron beam provided a complete decomposition of lithium carbonate, because no weight changes (without magnetic field) on TG curves were revealed.

Second, in the magnetic field at temperatures in the range (450–600) °C, the extended rise of the TG curve was observed that terminated with a weight jump at a temperature of 630 °C. This jump was caused by the magnetic phase transition at the Curie temperature ( $T_c$ ) in lithium pentaferriite when the force interaction with the external magnetic field terminated as a result of ferromagnetic phase transition into the paramagnetic state. The value  $T_c = 630$  °C is in agreement with the literature data [17] for lithium pentaferriite. With increasing duration of annealing, the jump monotonically increased, which testified to the lithium pentaferriite phase accumulation at 600 °C in the examined range of annealing times.

Third, an endothermic peak arose and increased on the DSC curves at ca. 753 °C caused by polymorphic transition of the ordered lithium pentaferriite  $\alpha$ -modification into the

**Fig. 5** Dependences of TG/DSC curves for reaction mixtures after  $T$  and RT ferritization at 750 °C



disordered  $\beta$ -modification [18]. This additionally confirmed the lithium pentaferriite formation during RT annealing.

The DTG dependences obtained by differentiation of the TG curves characterize more precisely and vividly the weight changes. The non-monotonic character of the TG curves for lithium pentaferriite at temperatures below  $T_c$  can be seen from the DTG dependences. In particular, after RT annealing for 120 min, the weakly expressed wide DTG peak can be identified at temperatures in the range (500–600) °C. This peak is most likely due to transitions of lithium ferrosphel doped by zinc into the paramagnetic state.

The decreased Curie temperature of lithium substituted ferrite is a consequence of the Néel theory according to which the diamagnetic substitution of tetrahedral iron cations by zinc ions leads to a strong decrease in the intersublattice exchange interaction, partial disorientation of the magnetic moments in domains, and decrease in the ferrite magnetization and its Curie temperature [19, 20].

The position of DTG temperature peaks in the magnetic field for the degree of substitution  $x$  of  $\text{Li}_{0.5(1-x)}\text{Zn}_x\text{Fe}_{2.5-0.5x}\text{O}_4$  lithium–zinc ferrite was established in [11]. Taking into account the data presented in [11] and considering that the wide peak is a superposition of several peaks, we obtain that a

set of phases of lithium-substituted ferrosphels with  $0 \leq x \leq 0.15$  is responsible for this peak. It should be noted that low intensity of low-temperature peaks is caused not only by small concentration of phases, but also by the natural decrease of phase magnetization with increasing degree of substitution  $x$ . This also follows from the Néel theory.

An increase in the ferritization annealing temperature up to 750 °C leads to an increased rate of synthesis in both ferritization regimes. From the thermograms in Fig. 5 it can be seen that simple thermal heating of the mixture to 750 °C without isothermal annealing does not lead to complete decomposition of lithium carbonate. However, after thermal annealing for  $\geq 10$  min, all possible features of accumulation of lithium pentaferriite phase and lithium-substituted ferrosphels listed above can be observed. Moreover, the amount of accumulated lithium ferrosphels increased in the entire interval of the examined annealing times. The data shown in Fig. 3 testify to the accelerated consumption of reagents at 750 °C and are in agreement with this statement.

The increased efficiency of synthesis during RT annealing at 750 °C is manifested as follows. From the DTG and DSC peak intensities, it can be seen that after 10 min annealing, the maximum lithium pentaferriite concentration comparable with the lithium pentaferriite

concentration reached after 120 min of  $T$  annealing is accumulated. With further increase in the annealing time, the intensity of the DTG and DSC peaks caused by the lithium pentaferriite decreases, but the intensity of the low-temperature DTG peaks caused by lithium-substituted ferros spinels significantly increases. For  $t_{\text{ann}} = 120$  min, we have the well pronounced DTG peak at ca. 490 °C; the position of this maximum corresponds to the Curie temperature of lithium–zinc ferrite with  $x = 0.2$  [11]. Since curves 4 in Fig. 3 testify to the termination of the reagent consumption for  $t_{\text{ann}} \leq 20$  min, it seems likely that the end-product, that is, the  $\text{Li}_{0.4}\text{Fe}_{2.4}\text{Zn}_{0.2}\text{O}_4$  phase is formed as a result of interaction of the intermediate lithium-substituted ferrite phases. Considering that the diffusion processes provide the basis for these interactions, we can conclude that the diffusion mass transfer is intensified in the accelerated electron beam.

## Conclusions

Our analysis of the kinetic changes in the phase composition of the reaction mixtures during thermal and radiation-thermal heating allows us to conclude the following:

- The initial prevailing phase formation process in the  $\text{Li}_2\text{CO}_3\text{--Fe}_2\text{O}_3\text{--ZnO}$  system is the decomposition of lithium carbonate with  $\text{CO}_2$  emission and formation of the  $\text{Li}_{0.5}\text{Fe}_{2.5}\text{O}_4$  pure weakly zinc-doped lithium pentaferriite phase. The radiation effect of intensification of solid-phase processes is most strongly manifested at this stage of synthesis.
- In the subsequent stages of annealing, the synthesis process occurs through the formation of the  $\text{Li}_{0.5(1-x)}\text{Zn}_x\text{Fe}_{2.5-0.5x}\text{O}_4$  ( $0 \leq x \leq 1$ ) intermediate spinel phases. The end-product is formed as a result of the diffusion interactions of phases. The electron beam causes the rate of such interaction to increase, especially when the reaction temperature increases to 750 °C.
- Local overheating of interphase boundaries at the expense of radiation-induced excitations of the electron subsystem that tend to annihilate non-radiatively on contacts of powder mixture particles can be a possible reason for the high efficiency of the initial stage of synthesis.

## References

1. Berbennia V, Marini A, Matteazzib P, Riccerib R, Welhamc NJ. Solid-state formation of lithium ferrites from mechanically activated  $\text{Li}_2\text{CO}_3\text{--Fe}_2\text{O}_3$  mixtures. *J Eur Ceram Soc.* 2003;23: 527–36.
2. Yasuoka M, Nishimura Y, Nagaoka T, Watari K. Influence of different methods of controlling microwave sintering. *J Therm Anal Calorim.* 2006;83:407–10.
3. Jugović D, Mitrić M, Cvjetičanin N, Jančar B, Mentus S, Uskoković D. Synthesis and characterization of  $\text{LiFePO}_4/\text{C}$  composite obtained by sonochemical method. *J Solid State Ionics.* 2008;179:415–9.
4. Zhang B, Chen G, Xu P, Lu Z. Effect of ultrasonic irradiation on the composition and electrochemical properties of cathode material  $\text{LiNi}_{0.5}\text{Mn}_{0.5}\text{O}_2$  for lithium batteries. *J Solid State Ionics.* 2007;178:1230–4.
5. Lyakhov NZ, Boldyrev VV, Voronin AP, Gribkov OS, Bochkarev LG, Rusakov SV, Auslender VL. Electron beam stimulated chemical reaction in solids. *J Therm Anal Calorim.* 1995;43: 21–31.
6. Surzhikov AP, Pritulov AM, Ivanov YF, Shabardin RS, Usmanov RU. Electron-microscopic study of morphology and phase composition of lithium-titanium ferrites. *Russian Phys J.* 2001;44: 420–3.
7. Baba PD, Argentina GM, Courtney WE, Dionne GF, Temme DH. Fabrication and properties of microwave lithium ferrites. *IEEE Trans Magn.* 1972;8:83–94.
8. Jiang XN, Lan ZW, Yu Z, Liu PY, Chen DZ, Liu CY. Sintering characteristics of  $\text{LiZn}$  ferrites fabricated by a sol–gel process. *J Magn Magn Mater.* 2009;321:52–5.
9. Surzhikov AP, Pritulov AM, Lysenko EN, Sokolovskii AN, Vlasov VA, Vasendina EA. Calorimetric investigation of radiation-thermal synthesized lithium pentaferriite. *J Therm Anal Calorim.* 2010;101:11–3.
10. Surzhikov AP, Sokolovskii AN, Vlasov VA, Vasendina EA. Synthesis of lithium-zinc ferrite in beam of accelerated electrons. *Rare Metals Spec Issue.* 2009;28:418–20.
11. Surzhikov AP, Lysenko EN, Vasendina EA, Sokolovskii AN, Vlasov VA, Pritulov AM. Thermogravimetric investigation of the effect of annealing conditions on the soft ferrite phase homogeneity. *J Therm Anal Calorim.* 2011;104:613–7.
12. Surzhikov AP, Pritulov AM, Lysenko EN, Sokolovskii AN, Vlasov VA, Vasendina EA. Influence of solid-phase ferritization method on phase composition of lithium–zinc ferrites with various concentration of zinc. *J Therm Anal Calorim.* 2011 (Online First).
13. Lin DM, Wang HS, Lin ML, Lin MH, Wu YC. TG(M) and DTG(M) techniques and some of their applications on material study. *J Therm Anal Calorim.* 1999;58:347–53.
14. Shiliakov SM, Maltsev VI, Ivolga VV, Naiden EP. Atomic composition of lithium–zinc–iron spinels. Reference *Izvestiya Vysshikh Uchebnykh Zavedenii, Moskva. Ser.: Fizika.* 1977; 111–16.
15. Tobón-Zapata GE, Ferrer GE, Etcheverry SB, Baran EJ. Thermal behavior of pharmacologically active lithium compounds. *J Therm Anal Calorim.* 2000;61:29–35.
16. Rama Rao S, Sunandana CS. Quenched lithium carbonate. *J Phys Chem Solids.* 1996;57:315.
17. SY An, Shim I-B, Kim CS. Synthesis and magnetic properties of  $\text{LiFe}_5\text{O}_8$  powders by a sol-gel process. *J Magn Magn Mater.* 2005;290:1551–4.
18. Ahniyaz A, Fujiwara T, Song S-W, Yoshimura M. Low temperature preparation of  $\beta\text{-LiFe}_5\text{O}_8$  fine particles by hydrothermal ball milling. *J Solid State Ionics.* 2002;151:419–23.
19. Gorter EW. Saturation magnetisation and crystal chemistry of ferrimagnetic oxides. *J Philips Res Rep.* 1954;9:295.
20. Smit J, Win HPJ. Ferrites, Physical properties of ferrimagnetic oxides in relation to their technical applications. Eindhoven: Philips Technical Library; 1959. p. 299.